JOHNSON, C. K. & LEVY, H. A. (1974). *International Tables for X-ray Crystallography*, Vol. IV, pp. 311–336. Birmingham: Kynoch Press. (Present distributor D. Reidel, Dordrecht.)
KOESTER, L. (1977). *Neutron Physics*, edited by G. HOHLER, p. 1. Berlin: Springer.
KROON, P. A. & VOS, A. (1979). *Acta Cryst.* A**35**, 675–684.
LEHMANN, M. S. & LARSEN, F. K. (1974). *Acta Cryst.* A**30**, 580–584.
MCCANDLISH, L. E., STOUT, G. H. & ANDREWS, L. C. (1975). *Acta Cryst.* A**31**, 245–249.
MCMULLAN, R. K. & KOETZLE, T. F. (1979). Unpublished.
MEULENAER, J. DE & TOMPA, H. (1965). *Acta Cryst.* **19**, 1014–1018.
NELMES, R. J. (1975). *Acta Cryst.* A**31**, 273–279.
PROUT, C. K. & WALLWORK, S. C. (1966). *Acta Cryst.* **21**, 449–450.
PULLMAN, B. (1964). *Acta Cryst.* **17**, 1074–1075.
REES, B. (1976). *Acta Cryst.* A**32**, 483–488.
SCHOMAKER, V. & TRUEBLOOD, K. N. (1968). *Acta Cryst.* B**24**, 63–76.
SPACKMAN, M. A. (1986). *J. Chem. Phys.* **85**, 6579–6586, 6587–6601.
SPACKMAN, M. A. (1987). *J. Phys. Chem.* **91**, 3179–3186.
SPACKMAN, M. A., WEBER, H. P. & CRAVEN, B. M. (1988). *J. Am. Chem. Soc.* In the press.
STEWART, R. F. (1972). *J. Chem. Phys.* **57**, 1664–1668.
STEWART, R. F. (1976). *Acta Cryst.* A**32**, 565–574.
STEWART, R. F. (1982). *God. Jugosl. Cent. Kristalogr.* **17**, 1–24.
STEWART, R. F. (1983). Unpublished.
STEWART, R. F. (1987). Unpublished.
STEWART, R. F., DAVIDSON, E. R. & SIMPSON, W. T. (1965). *J. Chem. Phys.* **42**, 3175–3187.
SWAMINATHAN, S., CRAVEN, B. M. & MCMULLAN, R. K. (1984). *Acta Cryst.* B**40**, 300–306.
SWAMINATHAN, S., CRAVEN, B. M. & MCMULLAN, R. K. (1985). *Acta Cryst.* B**41**, 113–122.
SWAMINATHAN, S., CRAVEN, B. M., SPACKMAN, M. A. & STEWART, R. F. (1984). *Acta Cryst.* B**40**, 398–404.
TEMPLETON, L. K. & TEMPLETON, D. H. (1973). Proc. Am. Crystallogr. Assoc. Meet., Storrs, CT, USA, Abstracts, p. 143.
WEBER, H. P. & CRAVEN, B. M. (1987). *Acta Cryst.* B**43**, 202–209.
WEBER, H. P., CRAVEN, B. M. & MCMULLAN, R. K. (1983). *Acta Cryst.* B**39**, 360–366.
WEBER, H. P., RUBLE, J. R., CRAVEN, B. M. & MCMULLAN, R. K. (1980). *Acta Cryst.* B**36**, 1121–1226.
WILLIS, B. T. M. (1970). *Acta Cryst.* A**26**, 396–401.

Acta Cryst. (1988). B**44**, 281–289

Single-Crystal X-ray Geometries and Electron Density Distributions of Cyclopropane, Bicyclopropyl and Vinylcyclopropane. I. Data Collection, Structure Determination and Conventional Refinements

BY DICK NIJVELDT AND AAFJE VOS

Laboratory of Chemical Physics, University of Groningen, Nijenborgh 16, 9747 *AG Groningen, The Netherlands*

(*Received* 21 *November* 1986; *accepted* 9 *December* 1987)

Abstract

Crystal structures of cyclopropane (CP) C_3H_6, bicyclopropyl (BCP) C_6H_{10} and vinylcyclopropane (VCP) C_5H_8 have been determined by accurate single-crystal X-ray measurements at $T \approx 100$ K. In addition to the conventional full-angle refinements [$(\sin\theta)/\lambda < 1{\cdot}15$ Å^{-1} for CP and $< 1{\cdot}22$ Å^{-1} for BCP and VCP], high-order refinements [$(\sin\theta)/\lambda > 0{\cdot}60$ Å^{-1} for CP, $> 0{\cdot}80$ Å^{-1} for BCP and $> 0{\cdot}70$ Å^{-1} for VCP] have been performed to obtain accurate parameters for C atoms. C_3H_6: CP molecules in the crystal approximate the D_{3h} symmetry of the free CP molecule; $M_r = 42{\cdot}08$, orthorhombic, $Cmc2_1$, $a = 7{\cdot}971$ (3), $b = 6{\cdot}575$ (3), $c = 5{\cdot}844$ (2) Å, $V = 306{\cdot}3$ (2) Å^3, $Z = 4$, $D_x = 0{\cdot}913$ Mg m^{-3}, λ(Mo $K\bar{\alpha}$) $= 0{\cdot}71069$ Å, $\mu = 0{\cdot}540$ cm^{-1}, $F(000) = 96$, $T = 94$ K, $R(F) = 0{\cdot}0328$ and $R_w(F) = 0{\cdot}0280$ for the full-angle refinement on 915 observed independent reflections. C_6H_{10}: The molecules in the crystal have the *trans*-bisected conformation; $M_r = 82{\cdot}15$, orthorhombic, $Cmca$, $a = 8{\cdot}8528$ (7), $b = 5{\cdot}0911$ (3), $c = 11{\cdot}7294$ (13) Å, $V = 528{\cdot}65$ (8) Å^3, $Z = 4$, $D_x = 1{\cdot}033$ Mg m^{-3}, λ(Mo $K\bar{\alpha}$) $= 0{\cdot}71069$ Å, $\mu = 0{\cdot}616$ cm^{-1}, $F(000) = 184$, $T = 100$ K, $R(F) = 0{\cdot}0389$ and $R_w(F) = 0{\cdot}0414$ for the full-angle refinement on 1817 observed independent reflections. C_5H_8: The molecules in the crystal deviate slightly from the *trans*-bisected conformation; $M_r = 68{\cdot}12$, monoclinic, $P2_1$, $a = 4{\cdot}8792$ (9), $b = 7{\cdot}1617$ (11), $c = 6{\cdot}9230$ (11) Å, $\beta = 105{\cdot}068$ (13)°, $V = 233{\cdot}60$ (7) Å^3, $Z = 2$, $D_x = 0{\cdot}968$ Mg m^{-3}, λ(Mo $K\bar{\alpha}$) $= 0{\cdot}71069$ Å, $\mu = 0{\cdot}579$ cm^{-1}, $F(000) = 76$, $T = 94$ K, $R(F) = 0{\cdot}0323$ and $R_w(F) = 0{\cdot}0395$ for the full-angle refinement on 3480 observed independent reflections.

1. Introduction

The present study is focused on volatile compounds containing one or two three-membered carbon rings. In addition to the parent compound cyclopropane (CP) C_3H_6, the two derivatives bicyclopropyl (BCP) C_6H_{10} and vinylcyclopropane (VCP) C_5H_8 will be considered (for structural formulae, see Fig. 3). CP is a gas and BCP and VCP are liquids at room temperature.

0108-7681/88/030281-09$03.00

The selected compounds are of interest because the bonding character of the cyclopropyl group deviates strongly from the bonding character of acyclic (saturated) hydrocarbons; the cyclopropyl group shows a strong similarity with ethene. The unsaturated character of CP allows conjugation between the two cyclopropyl groups in BCP, or between the cyclopropyl group and the unsaturated vinyl group in VCP. A major aim of the present work is to investigate possible influences of conjugation on the molecular geometry and on the electron density distribution in BCP and VCP. Since these effects are expected to be small, especially for BCP, their determination demands very accurate measurement. Prior to the underlying study, neither a very accurately measured geometry nor electron density distribution was available for CP, BCP or VCP. Because exact determination of the geometry and thermal motion by neutron diffraction would have required large high-quality crystals of the volatile compounds at a neutron diffraction centre, it was decided to base the geometry and electron density determination on X-ray diffraction intensities only. Major topics of the present study are: crystallization and accurate data collection (present paper), multipole refinements and dynamic deformation densities [Nijveldt & Vos (1988*a*); hereinafter referred to as paper II] and theoretical and experimental evidence for conjugation in BCP and VCP [Nijveldt & Vos (1988*b*); hereinafter referred to as paper III].

2. Previous geometrical studies

2.1. *VCP*

For VCP, structure determinations of the solid phase have not been published. The studies available for VCP in solution or in the gas phase show a clear preference for the *trans*-bisected conformation, but do not give detailed information on the molecular geometry [^{1}H NMR: De Maré & Lapaille (1980); electron diffraction: Trætteberg (1983); Raman: Carreira, Towns & Malloy (1978)].

2.2. *CP*

Several studies of the solid phase are available; only the most recent ones will be discussed. Bates, Sands & Smith (1969) reported an X-ray diffraction study in combination with infrared and Raman spectra of polycrystalline CP at 85 K. To index their 15 powder lines they used the results from a single-crystal infrared investigation by Brecher, Krikorian, Blanc & Halford (1961), in which an orthorhombic crystal system was predicted with molecules positioned at sites with mirror-plane symmetry. The cell chosen by Bates *et al.* is primitive with unit-cell axes of 10·0, 6·8 and 5·1 Å. The decision whether or not the crystals contain inversion centres was hampered by the limited accuracy of the Raman data. A more recent study of Raman and infrared spectra of polycrystalline CP by Bertie & Jacobs (1977) indicated the point group to be non-centrosymmetric, C_{2v}.

2.3. *BCP*

Eraker & Rømming (1967) have measured 307 independent X-ray reflections with the multifilm technique on a cylindrically shaped single crystal at 170 K. The crystal system is orthorhombic, space group *Cmca*, $a = 8{\cdot}904$ (7), $b = 5{\cdot}137$ (4), $c = 11{\cdot}807$ (5) Å, and $Z = 4$. The molecules are located at special positions with $2/m$ symmetry and are consequently in the *trans*-bisected conformation.

3. Crystallization

The present crystallization method is based on the procedure developed for gaseous compounds by van Nes & van Bolhuis (1978). Especially for the liquid samples, modifications have been applied. The two types of capillaries, designed for gaseous and liquid samples, are depicted in Fig. 1.* In these capillaries, the high-quality spherical crystals have been grown *in situ* on the CAD-4 diffractometer. Information on the physical properties of the three compounds is included

* A report on the filling of the capillaries and the crystallization of the compounds has been deposited with the British Library Document Supply Centre as Supplementary Publication No. SUP 44633 (9 pp.). Copies may be obtained through The Executive Secretary, International Union of Crystallography, 5 Abbey Square, Chester CH1 2HU, England.

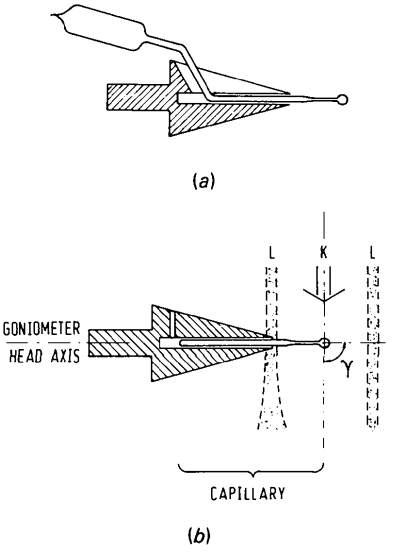

Fig. 1. Side view of capillaries attached to their mounting cone. (*a*) Capillary for gaseous CP. (*b*) Capillary for the liquids BCP and VCP. Cooling is performed by a cold vertical N_2 gas stream (*K*), which is surrounded by a room-temperature N_2 gas stream (*L*).

Table 1. *Crystal data*

	CP-I	CP-II	CP	BCP	VCP
Formula	C_3H_6	C_3H_6	C_3H_6	C_6H_{10}	C_5H_8
Boiling point (K)	240	240	240	349	313
Melting point (K)	145	145	145	191	161
Crystallization temperature (K)	132·0 (10)	131·0 (10)	—	153·0 (10)	143·0 (10)
Measuring temperature (K)	94·0 (10)	94·0 (10)	—	100·0 (10)	94·0 (10)
Crystal diameter (mm)	0·500 (10)	0·500 (10)	—	0·505 (10)	0·568 (10)
Mosaic spread (°)	≤ 1·9	≤ 1·2	—	≤ 0·4	≤ 0·4
μ(Mo $K\bar{\alpha}$) (cm^{-1})	0·540	0·540	—	0·616	0·579
Radiation wavelength (Å)	0·71069	0·71069	—	0·71069	0·71069
Tube voltage (kV)	50	50	—	50	50
Tube current (mA)	24	24	—	32	32
Crystal: counter speed	1:0	1:0	—	1:1	1:1
Crystal scan angle (°)	2·8 + 0·43 tanθ	2·0 + 0·43 tanθ	—	1·0 + 0·43 tanθ	1·0 + 0·50 tanθ
Slit width, horizontal (mm)	2·7 + 2·60 tanθ	2·2 + 2·60 tanθ	—	2·2 + 1·30 tanθ	2·3 + 1·30 tanθ
Slit width, vertical (mm)	6·0	4·9	—	4·0	4·0
Scan speed (° min^{-1})	0·5	0·5	—	0·5	0·5
Misalignment limit (°)	0·10	0·10	—	0·05	0·05
Multiple reflection χ	4·6	4·6	—	3·0	3·0
First χ test passed (%)	75	83	—	75	65
$(\sin\theta_{max})/\lambda$ 1st part (Å^{-1})*	1·15	1·15	—	1·22	1·22
$(\sin\theta_{max})/\lambda$ 2nd part (Å^{-1})*	1·15	1·15	—	1·22	1·22
$(\sin\theta_{max})/\lambda$ 3rd part (Å^{-1})*	1·08	0·48	—	0·48	0·48
$(\sin\theta_{max})/\lambda$ 4th part (Å^{-1})*	1·08	0·48	—	—	—
Measuring time (weeks)	2·5	2	—	3	6
Total drop I (references) (%)	3·1	2·5	—	3·1	5·2
Total number of reflections	3369	2405	—	4495	9062
Internal consistency $R_w(I)$ (%)	1·307	1·073	0·952	1·175	0·966
Number of independent reflections	1072	1073	1073	2077	3670
Number of extincts	90	88	79	130	95
κ (cutoff for less-thans)	—	—	1·92	1·84	1·45

* Unique part of reciprocal space; octant for CP and BCP, quadrant for VCP.

in Table 1. For the experiments the following samples have been used.

(*a*) CP gas, commercially available from Fluka A.G., with a quoted impurity ≤ 2%.

(*b*) Liquid BCP and VCP with a quoted impurity ≤ 0·1%. Ampoules containing 1·8 g of each of the samples were kindly supplied by Professor Dr W. Lüttke, University of Göttingen, Federal Republic of Germany. BCP was synthesized according to the procedures of Furukawa, Kawabata & Nishimura (1968) and de Meijere, Schallner & Weitemeyer (1973). VCP was prepared according to Kirmse, Von Bülow & Schepp (1966).

4. Data collection

Much emphasis is put on the intensity measurements in order to obtain an extensive and accurate set of structure factors for the determination of a reliable deformation density distribution. A large number of reflections with a significant intensity at high $(\sin\theta)/\lambda$ is needed to minimize parameter correlation during the least-squares refinements. Random errors are kept small and precautions are taken to reduce systematic errors as much as possible. An Enraf–Nonius CAD-4F diffractometer has been used for the intensity measurements. Numerical information about data collection is presented in Table 1. CP-I and CP-II refer to different CP crystals obtained from the same gaseous sample.

4.1. *Precautions and conditions*

Crystal quality. Spherically shaped crystals have been taken to avoid corrections for absorption and for inhomogeneity of the primary-beam intensity distribution (§4.2). Diameters and linear absorption coefficients μ(Mo $K\bar{\alpha}$) are included in Table 1. The maximum variation in transmission coefficient, from 0·97566 at $\theta = 0°$ to 0·97577 at $\theta = 90°$ for VCP is 0·01% if the crystal is bathed in a uniform X-ray beam (*cf.* §4.2).

Much care was taken, in the crystallization stage, to obtain crystals with a small mosaic spread. The mosaic spread has been defined as the width of the intensity profile at 1% of the peak height, measured on a low-order reflection by means of an ω scan and application of the smallest available horizontal counter opening (0·25 mm). For each of the crystals, Table 1 includes the maximum value of the mosaic spread obtained from measurements at different azimuth angles on three reflections with mutually orthogonal diffraction vectors. The mosaic spread was checked regularly during data collection, but no increase of the initial values was observed.

Cooling. Crystal-temperature control has been treated in the report of the improved crystallization method (*cf.* deposition footnote). By means of a thermocouple voltage, the temperature of the cold-gas stream was recorded on paper continuously during data collection and sampled and stored on disk for each

Table 2. *Cell parameters at crystallization and measuring temperature*

Compound	T (K)	a (Å)	b (Å)	c (Å)	β (°)	V (Å^3)
CP-II	131·0 (10)	7·970 (5)	6·540 (2)	6·011 (3)		313·3 (3)
CP-II	94·0 (10)	7·971 (3)	6·575 (3)	5·844 (2)		306·3 (2)
BCP	153·0 (10)	8·844 (3)	5·161 (2)	11·753 (3)		536·4 (3)
BCP	100·0 (10)	8·8528 (7)	5·0911 (3)	11·7294 (13)		528·65 (8)
VCP	143·0 (10)	4·9032 (4)	7·1975 (7)	6·9804 (5)	105·580 (7)	237·29 (3)
VCP	94·0 (10)	4·8792 (9)	7·1617 (11)	6·9230 (11)	105·068 (13)	233·60 (7)

reflection (CAD-4 software modification by Dr J. L. de Boer, Department of Inorganic Chemistry, University of Groningen).

Changes in crystal alignment, caused by temperature fluctuations of the crystal mounting system, have been reduced by thermal isolation of the cone and goniometer head with thin layers of polystyrene. Moreover, excessive cooling of the mounting system was avoided by measuring the intensities at $80 < \gamma < 130°$ (see Fig. 1*b*). Alignment changes were most serious for CP (accepted misalignment 0·10° during alignment check) for which the capillary and mounting-cone configuration was not rotationally symmetric about the goniometer-head axis (*cf.* Fig. 1*a*).

Cell parameters. The cell parameters at measuring temperature (Table 2) have been determined from the four setting angles of each of 25 reflections by a least-squares fit of calculated to optimized values. The 25 reflections are randomly distributed over a $(\sin\theta)/\lambda$ shell with $(\sin\theta)/\lambda$ ranging from 0·60 to 0·70 Å^{-1} for CP and from 0·70 to 0·80 Å^{-1} for BCP and VCP. Differences between cell parameters at measuring and crystallization temperature (Table 2) can be explained by thermal expansion.

4.2. *Intensity measurements*

X-ray beam and scan method. The primary Mo $K\bar{\alpha}$ beam is flattened with a glass rod positioned horizontally between crystal and graphite monochromator (Helmholdt & Vos, 1977). In the crystal area, with diameter 0·5 mm, the resulting intensity distribution is homogeneous within ±4%.

The wavelength spread has been determined by performing an ω–2θ scan with narrow counter slit (0·25 mm) at $(\sin\theta)/\lambda = 1·0$ Å^{-1} on a small forsterite crystal (Mg_2SiO_4, $\varnothing = 0·11$ mm). At 2% of the intensity peak height the relative width of the reflection profile $\Delta\lambda/\lambda = 0·0074$.

Random errors (due to counting statistics) and systematic errors (due to nonlinear background below the peak) in the net intensities are reduced by keeping the background small. This has been accomplished by collimation of incident (source nozzle with $\varnothing =$ 0·9 mm) and diffracted (standard Enraf–Nonius detector collimator) beams (de Boer, 1982). Moreover, the scan method giving on average for the complete $(\sin\theta)/\lambda$ region the smallest counter aperture and thus the smallest background was adopted. Calculated values for crystal scan angle (from wavelength spread, divergence primary beam, crystal diameter and mosaic spread) and counter aperture (from scan-angle parameters plus adopted scan method) were checked and readjusted when necessary by a study of the profiles of those low- and high-order reflections which show the largest mosaic spread. Applied apparatus settings are listed in Table 1.

Standard deviations, scan speed and $(\sin\theta)/\lambda$ limits. For the CAD-4 diffractometer the ratio of the measuring time for peak intensity I_{pk} and background intensity I_{bg} is 2:1. The net intensity I is given by $I = I_{pk} - 2I_{bg}$. According to Rees (1976) the standard deviation of $\sigma(I^{1/2})$ due to counting statistics reads

$$\sigma(I^{1/2}) = \sigma(I)/(2I^{1/2}) = \tfrac{1}{2}[(I_{pk} + 4I_{bg})/(I_{pk} - 2I_{bg})]^{1/2} \quad \text{for } I > \sigma(I) \quad (1a)$$

and

$$\sigma(I^{1/2}) = \sigma^{1/2}(I)/2 = \tfrac{1}{2}(I_{pk} + 4I_{bg})^{1/4} \quad \text{for } I < \sigma(I). \quad (1b)$$

For $I > \sigma(I)$, $\sigma(I^{1/2})$ approximates the minimum value of 0·5 for $I_{bg} \ll I_{pk}$. Apart from scan speed and Lorentz and polarization factors, $\sigma(I^{1/2})$ is proportional to $\sigma[F_o(\mathbf{H})]$.

During the measurements the fixed-speed rather than the fixed-count procedure has been applied as this keeps, especially for stronger reflections, the variation in $\sigma[F_o(\mathbf{H})]$ small. This is favourable for the present electron density study, since least-squares refinements on $|F(\mathbf{H})|$ in which all reflections are included with equal weights and thus equal $\sigma[F_o(\mathbf{H})]$'s minimize $\int(\rho_o - \rho_c)^2 d\mathbf{r}$ (Wilson, 1976). For the different crystals equal angular velocities have been taken.

The high-order limit in $(\sin\theta)/\lambda$ is set by a desired value of $\sigma(I)/I \leq 2\%$ for the strongest high-order reflections. No overlap of intensity profiles occurs at the limits considered. Table 1 includes for each of the compounds $(\sin\theta)/\lambda$ limit, unique parts of reciprocal space measured, and measuring time for the complete data collection.

Multiple reflection. Multiple reflection is most drastic when strong reflections are involved (see *e.g.* Coppens, 1968). Errors due to this effect have been reduced by measuring each low-order reflection up to $(\sin\theta)/\lambda$

$= 0{\cdot}48$ Å^{-1} at three different azimuth angles ψ_i ($\Delta\psi = 0{\cdot}5°$). The multiple-reflection test reads

$$[\sum_{i=1}^{3}(\langle I\rangle - I_i)^2]/[\tfrac{1}{3}\sum_{i=1}^{3}\sigma_c^2(I_i)] \leq \chi, \qquad (2)$$

where $\sigma_c^2(I_i)$ is the variance based on counting statistics in the intensity of the ith measurement and χ is a freely selectable number. If the triplet passes the test, the ψ region is accepted and the ultimate intensity measurement is performed at the average azimuth angle. If the triplet is rejected, the procedure is repeated at another set of azimuth angles until a triplet of intensities satisfies (2). Table 1 shows that *ca* 25% of the reflections need more than one triplet.

Intensity and orientation control. For each crystal, three low-order reflections with mutually orthogonal diffraction vectors and $I > 100\sigma(I)$ have been measured every 1·5 h as intensity-control reflections. The reference intensities show an almost linear decrease in time. For each crystal, Table 1 gives the average drop of the reference intensities during the period of data collection. Within each of the measuring series corrections deduced from the reference reflections are smaller than 2%. The drop in reference intensity has been ascribed mainly to the high 'operating age' of the X-ray tube (Philips, Mo, 2kW, fine focus). The 'operating age' at the measurements, which are performed in the sequence BCP, VCP, CP-I and CP-II, runs from 60 to 120 weeks. Reference intensity measurements on forsterite, carried out between the data collections, yield an average drop in the primary-beam intensity of roughly 1% per week.

For each measuring series, three orientation-control reflections with $(\sin\theta)/\lambda \approx 0{\cdot}70$ Å^{-1} have been selected in the relevant part of the reciprocal space to check the alignment of the crystal after every 50 measured reflections. The criterion for alignment is determined by the 'misalignment limit', *viz* the angle between the observed scattering vector and the scattering vector derived from the crystal-orientation matrix. If this limiting value (see Table 1) is exceeded, a new matrix is calculated on the basis of 22 reoptimized reorientation reflections.

Strong reflections. To prevent intensity errors, caused by the non-linearity of the counter circuit (counter deadtime: 1μs) or by the use of an attenuation filter, strong reflections have been removed from the reflection list and remeasured at a reduced tube current. In this way deadtime errors larger than 1% of the integrated intensity are avoided.

Apparatus instability. Instabilities observed by van der Wal (1982, p. 106) during data collection on forsterite also affect the present intensity measurements. Repeated measurement of the (strong) $30\bar{1}$ reflection of VCP with a statistical accuracy $\sigma_c(I)/I = 0{\cdot}15\%$ reveal intensity differences up to 7%. The root-mean-square deviation of the repeatedly measured intensity amounts to 2%. This large instability, ascribed to irregularities in the motor speed, has been removed recently by an extensive mechanical revision of the diffractometer by Enraf–Nonius.

Note that irregularities in motor speed have the largest effect on the integrated intensities of strong reflections with steep profiles, like the VCP $30\bar{1}$ reflection mentioned above. For high-order reflections and for moderate and weak low-order reflections the error due to apparatus instability is considerably smaller.

5. Data reduction

5.1. *Scaling and averaging of reflection intensities*

For each unique part of reciprocal space (octant or quadrant) the collected reflections were divided into different series to cope with the special treatment of low-order reflections (multiple reflection; strong reflections) and with limitations in the storage capacity of the disk unit (complete reflection profiles are stored). Different series have at least 50 reflections in common. All series, belonging to one crystal, are put on the same scale according to the procedure of Hamilton, Rollett & Sparks (1965), in which symmetrically related reflections are treated as identical reflections. After this the weighted average intensity $\langle I(\mathbf{H})\rangle_w$ is calculated for each independent reflection **H** according to

$$\langle I(\mathbf{H})\rangle_w = [\sum_{i=1}^{n(\mathbf{H})} w_{c,i}(\mathbf{H})I_i(\mathbf{H})]/\sum_{i=1}^{n(\mathbf{H})} w_{c,i}(\mathbf{H}),$$

where $n(\mathbf{H})$ is the number of measurements for reflection **H** and $w_{c,i}(\mathbf{H})$ is the weight based on counting statistics. The weighted internal consistency factor of the sets of identical reflections

$$R_w(I) = (\{\sum_{\mathbf{H}}\sum_{i=1}^{n(\mathbf{H})} w_{c,i}(\mathbf{H})[\langle I(\mathbf{H})\rangle_w - I_i(\mathbf{H})]^2\}$$

$$\times \{\sum_{\mathbf{H}}\sum_{n=1}^{n(\mathbf{H})} w_{c,i}(\mathbf{H})[I_i(\mathbf{H})]^2\}^{-1})^{1/2},$$

included in Table 1, is approximately 1% for each of the crystals. Finally, scaling and averaging of the two different series for CP, CP-I and CP-II, according to the above-mentioned procedure gave the final CP set. $\langle I(\mathbf{H})\rangle_w$, hereafter shortly referred to as $I(\mathbf{H})$, has been adopted as the best intensity for the independent reflection **H**.

Since the standard deviation based on counting statistics represents only a part of the possible error in $I(\mathbf{H})$, $\sigma[I(\mathbf{H})]$ is taken equal to the largest of the quantities

$$\sigma_c[I(\mathbf{H})] = [\sum_{i=1}^{n(\mathbf{H})} w_{c,i}(\mathbf{H})]^{-1/2}$$

Table 3. *Crystallographic data at measuring temperature*

	CP	BCP	VCP
Crystal system	Orthorhombic	Orthorhombic	Monoclinic
Systematic extinctions	*hkl*: $h+k\neq 2n$ *h0l*: $l\neq 2n$	*h0l*: $l\neq 2n$ *hk0*: $h\neq 2n$ *hk0*: $h\neq 2n$	0*k*0: $k\neq 2n$
Space group adopted	$Cmc2_1$	*Cmca*	$P2_1$
Molecular site symmetry	*m*	2/*m*	1
Z	4	4	2
D_x (Mg m^{-3})	0·913	1·033	0·968
F(000) (electrons)	96	184	76

and

$$\sigma_v[I(\mathbf{H})] = (\{\sum_{i=1}^{n(\mathbf{H})} [I(\mathbf{H})-I_i(\mathbf{H})]^2\}/\{n(\mathbf{H})[n(\mathbf{H})-1]\})^{1/2}.$$

5.2 *Observed structure factors*

Corrections for Lorentz and polarization factors have been applied to $I^{1/2}$ and $\sigma(I^{1/2})$ to obtain $|F_o(\mathbf{H})|$ and $\sigma[F_o(\mathbf{H})]$ on a relative scale. Reflections with negative net intensity (extincts) and weak reflections with $|F_o(\mathbf{H})| \leq \kappa\sigma[F_o(\mathbf{H})]$ (less-thans) have been excluded from the least-squares refinements. To reduce parameter biases due to these omissions as much as possible, κ is chosen in such a way that the numbers of extincts and less-thans are equal. In all cases, $\kappa < 2{\cdot}0$ (Table 1).

6. Space groups and approximate structure models

Crystal system, systematic extinctions and the space groups adopted for each of the compounds, are listed in Table 3. The number of molecules per cell *Z* agrees with a density of approximately 1 Mg m^{-3}. Patterson syntheses reveal the absence of a mirror plane in CP perpendicular to **c** and in VCP perpendicular to **b**. The BCP model reported by Eraker & Rømming (1967) with space group *Cmca* was adopted in the present study. For CP the selected space group agrees with the point group C_{2v} found by Bertie & Jacobs (1977), the cell dimensions deviate strongly from the ones reported by Bates *et al.* (1969). The CP molecule lies at a mirror plane perpendicular to **a**. BCP contains, in addition to a mirror plane perpendicular to **a**, an inversion centre at the central bond. The VCP molecule is located at a general position.

7. Refinements with spherical scattering factors for carbon

7.1. *Full-angle refinements*

Least-squares refinements have been carried out with the *VALRAY* system (Stewart & Spackman, 1981). The function minimized is $Q = \sum_{\mathbf{H}} w(\mathbf{H})|F_o(\mathbf{H})-\mathrm{Sc}\,F_c(\mathbf{H})|^2$. The spherical scattering factor for C atoms is deduced from Clementi's (1965) analytical SCF atomic orbitals of the atom in its ground state. For the positional free H atom, the 'polarized H atom' (paper II, §2.1) has been chosen with scattering factors from Stewart, Bentley & Goodman (1975). Anisotropic thermal tensors **U** have been taken into account for C atoms and isotropic thermal parameters $\langle u^2\rangle$ for H atoms. No corrections for extinction have been considered. In CP and VCP, shifts of the molecules as a whole along the polar twofold screw axis have been avoided by fixing, along this axis, the coordinate of the C atom with the smallest thermal motion. The anisotropic temperature factor is

$$T(\mathbf{H}) = \exp[-2\pi^2(h^2a^{*2}U_{11} + k^2b^{*2}U_{22} + l^2c^{*2}U_{33} + 2hka^*b^*U_{12} + 2hla^*c^*U_{13} + 2klb^*c^*U_{23})]$$

and the isotropic temperature factor is

$$T_{\mathrm{iso}}(\mathbf{H}) = \exp[-8\pi^2\langle u^2\rangle(\sin\theta)^2/\lambda^2].$$

The weights during the refinement are $w(\mathbf{H}) = 0$ for $|F_o(\mathbf{H})| \leq \kappa\sigma[F_o(\mathbf{H})]$, and $w(\mathbf{H}) = m(\mathbf{H})$, reflection multiplicity, for $|F_o(\mathbf{H})| > \kappa\sigma[F_o(\mathbf{H})]$, where κ is the cutoff parameter defined in §5.2. The residuals are given by

$$R = [\sum_{\mathbf{H}} ||F_o(\mathbf{H})|-\mathrm{Sc}\,|F_c(\mathbf{H})||][\sum_{\mathbf{H}} |F_o(\mathbf{H})|]^{-1}$$

and

$$R_w = \{[\sum_{\mathbf{H}} w(\mathbf{H})||F_o(\mathbf{H})|-\mathrm{Sc}\,|F_c(\mathbf{H})||^2] \times [\sum_{\mathbf{H}} w(\mathbf{H})|F_o(\mathbf{H})|^2]^{-1}\}^{1/2}$$

Data concerning the full-angle (FA) refinements are listed in Table 4; the correlation coefficients between the different refined parameters do not exceed 0·70.

7.2. *High-order refinements, parameters of* C *atoms*

High-order (HO) refinements are performed to obtain the most reliable positional parameters for C atoms, with use of spherical scattering factors. After a series of refinements with different lower bounds in $(\sin\theta)/\lambda$, the value of $(\sin\theta_{\min})/\lambda$, given in Table 4, was determined for each of the compounds. The bound is taken as high as possible, under the condition that the HO region must contain a sufficiently large number of observed reflections. The scale factor was constrained to its FA

Table 4. *Results of the refinements with spherical scattering factors for* C *atoms*

N_o is the number of observed independent reflections and N_v the number of parameters considered. The other column headings are defined in the text. The units are: $(\sin\theta)/\lambda$ (Å^{-1}), R (%) and U_{eq} (10^{-5} Å^2).

$$U_{eq} = \tfrac{1}{3}\sum_i\sum_j U_{ij}a_i^*a_j^*\mathbf{a}_i.\mathbf{a}_j.$$

	Type	$(\sin\theta_{min})/\lambda$	$(\sin\theta_{max})/\lambda$	N_o	N_v	Sc	R	R_w	$\langle U_{eq}\rangle_C$
CP	FA	0·10	1·15	915	29	1·0000 (15)	3·28	2·80	2597
	HO	0·60	1·15	750	28	1·0000	4·11	4·59	2586
BCP	FA	0·08	1·22	1817	27	1·0051 (15)	3·89	4·14	1951
	HO	0·80	1·22	1241	26	1·0051	4·63	5·51	1962
VCP	FA	0·07	1·22	3480	77	0·9999 (10)	3·23	3·95	2029
	HO	0·70	1·22	2759	76	0·9999	2·94	3·20	2036

value to avoid correlation between this parameter and the thermal parameters, as a result of the restricted HO $(\sin\theta)/\lambda$ interval. H atoms were refined in the same way as during the FA refinements.

Data of the HO refinements are given in Table 4; the corresponding atomic parameters are specified in Table 5. No correlation coefficients larger than 0·70 have been found.

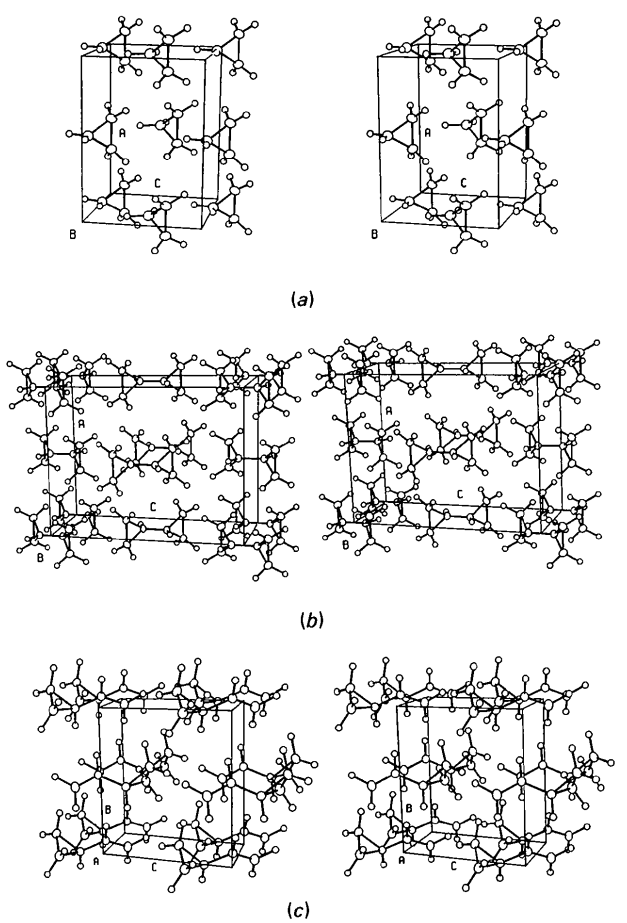

Fig. 2. Stereographic packing diagrams. (*a*) CP viewed down **b**. (*b*) BCP viewed down **b**. (*c*) VCP viewed down **a**.

8. Crystal packing and intermolecular interaction

The geometry description is based on the results of the ultimate multipole (UM) refinements (paper II, §2.7), since the standard deviations of the UM C-atom parameters are smaller than the corresponding HO values given in the previous section. The difference between corresponding HO and UM positional parameters for C atoms never exceeds the value of 1·5 times its estimated σ.

Pictures of the packing in the crystals and of the individual molecules are given in Figs. 2 and 3. Details of the molecular geometry will be given and discussed in paper III. The present discussion is restricted to the crystal packing and possible molecular deformations due to intermolecular interaction.

In CP, the molecules are located at mirror planes with heights $x = 0$ and $x = \frac{1}{2}$. These mirror planes bisect the endocyclic angle at C(1). The shortest intermolecular distances are C···C = 3·754 (2), C···H = 2·926 (8) and H···H = 2·639 (12) Å. In addition to the crystallographic mirror plane the mirror plane perpendicular to the threefold axis of the free-molecule point group D_{3h} is retained in the crystal. Since the two independent H—C—H angles differ by 3·9 (14)° it is possibly significant that the remaining symmetry elements of D_{3h} are lost in the crystallographic state.

In BCP the molecules lie at special positions with site symmetry $2/m$ and centres at $x = 0$ and $x = \frac{1}{2}$. The molecular site symmetry corresponds with the *trans*-bisected conformation of the molecule. The smallest intermolecular distances have values of 3·814 (1) for C···C, 3·125 (6) for C···H and 2·611 (8) Å for H···H.

The VCP molecules are located at general positions. The molecules are surrounded at shorter distances by their neighbours than in CP and BCP; smallest distances are C···C = 3·623 (1), C···H = 2·704 (7) and H···H = 2·553 (11) Å. The molecular conformation deviates slightly from the pure *trans*-bisected form, observed by ED in the gas phase, implying that the mirror symmetry with respect to the C(1)C(4)C(5) plane is not retained in the crystal. This deflection, probably due to intermolecular interactions, is demonstrated by the value of the dihedral angle $\tau = M-$

Table 5. *Fractional atomic coordinates* ($\times 10^5$) *and thermal parameters* ($Å^2 \times 10^5$) *of the high-order carbon skeleton*

		x	y	z	U_{11}	U_{22}	U_{33}	U_{12}	U_{13}	U_{23}	U_{eq}
CP	C(1)	0	30566 (12)	0	2372 (20)	2501 (20)	2761 (24)	0	0	452 (22)	2545 (12)
	C(2)	9407 (6)	17935 (9)	17053 (18)	1903 (10)	2963 (15)	2955 (16)	146 (12)	−220 (14)	291 (19)	2607 (8)
BCP	C(1)	0	−330 (7)	6364 (3)	1960 (9)	1441 (7)	1526 (8)	0	0	−10 (6)	1642 (5)
	C(2)	8493 (4)	20387 (7)	12898 (3)	2013 (8)	2292 (9)	2060 (8)	−131 (7)	−315 (7)	−412 (7)	2122 (5)
VCP	C(1)	8059 (5)	−1490	−21374 (4)	1577 (6)	1618 (6)	1637 (6)	0 (6)	432 (5)	21 (6)	1608 (3)
	C(2)	−2475 (8)	11572 (7)	−38958 (5)	2369 (10)	2170 (9)	1855 (8)	−158 (8)	470 (7)	440 (8)	2146 (5)
	C(3)	−23137 (6)	−614 (7)	−32128 (5)	1593 (7)	2586 (11)	2085 (8)	−189 (8)	325 (6)	147 (9)	2116 (5)
	C(4)	17769 (7)	6520 (6)	−1145 (4)	1969 (7)	1747 (7)	1710 (7)	70 (6)	344 (6)	−87 (6)	1834 (4)
	C(5)	39470 (9)	3 (8)	13225 (6)	2524 (11)	2511 (12)	1994 (9)	72 (10)	−138 (8)	103 (9)	2478 (6)

C(1)–C(4)–C(5) in which M is the centre of the distal bond C(2)–C(3). τ is 177·80 (5)° rather than the value of 180·00° observed for the *trans*-bisected conformation. Moreover, C(1) deviates by 0·0039 (6) Å from the plane perpendicular to the isosceles triangle C(2)C(4)C(3) and bisecting the inner angle at C(4).

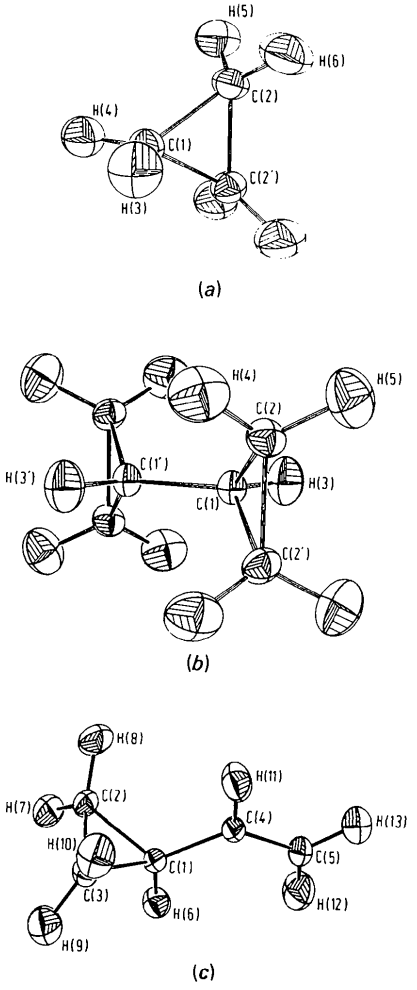

Fig. 3. Enlarged drawings of the molecules given in Fig. 2, with numbering of the atoms. Thermal ellipsoids from the UM model are given at 50% probability level (Johnson, 1976). (*a*) CP with $x(Cl) = 0$ and $z(Cl) = 0$. (*b*) BCP with centre at the cell origin. (*c*) VCP with $y(C5) = 0$.

In BCP and VCP, the molecular form found in the crystal corresponds with a low-energy conformation in the gas phase [*cf.* for BCP: the ED study by Hagen, Hagen & Trætteberg (1972) and for VCP: §2]. For the free molecules the *trans*-bisected conformation has the lowest energy in VCP and the second lowest in BCP.

The authors are grateful to Allan Forbes Cameron, University of Glasgow, Scotland, for his cooperation during the refinements on cyclopropane. Jan L. de Boer provided invaluable support during the data collections on the CAD-4 diffractometer. The computations were carried out at the Computing Centre of the University of Groningen. The investigations were supported in part by the Netherlands Foundation for Chemical Research (SON) with financial aid from the Netherlands Organization for the Advancement of Pure Research (ZWO).

References

BATES, J. B., SANDS, D. E. & SMITH, W. H. (1969). *J. Chem. Phys.* **51**, 105–112.

BERTIE, J. E. & JACOBS, S. M. (1977). *J. Chem. Phys.* **67**, 4981–4982.

BOER, J. L. DE (1982). In *Crystallographic Statistics*, edited by S. RAMASESHAN, M. F. RICHARDSON & A. J. C. WILSON, pp. 179–186. Madras: MacMillan India Press.

BRECHER, C., KRIKORIAN, E., BLANC, J. & HALFORD, R. S. (1961). *J. Chem. Phys.* **35**, 1097–1108.

CARREIRA, L. A., TOWNS, T. G. & MALLOY, T. B. (1978). *J. Am. Chem. Soc.* **100**, 385–388.

CLEMENTI, E. (1965). *Tables of Atomic Functions*. San José Research Laboratory, International Business Machines Corporation, San José, California, USA.

COPPENS, P. (1968). *Acta Cryst.* A**24**, 253–257.

DE MARÉ, G. R. & LAPAILLE, S. (1980). *Org. Magn. Reson.* **13**, 75–76.

ERAKER, J. & RØMMING, C. (1967). *Acta Chem. Scand.* **21**, 2721–2726.

FURUKAWA, J., KAWABATA, N. & NISHIMURA, J. (1968). *Tetrahedron*, **24**, 53–58.

HAGEN, K., HAGEN, G. & TRÆTTEBERG, M. (1972). *Acta Chem. Scand.* **26**, 3649–3661.

HAMILTON, W. C., ROLLETT, J. S. & SPARKS, R. A. (1965). *Acta Cryst.* **18**, 129–130.

HELMHOLDT, R. B. & VOS, A. (1977). *Acta Cryst.* A**33**, 456–465.

JOHNSON, C. K. (1976). *ORTEP*II. Report ORNL-5138. Oak Ridge National Laboratory, Tennessee, USA.
KIRMSE, W., VON BÜLOW, B. & SCHEPP, H. (1966). *Justus Liebigs Ann. Chem.* **691**, 41–49.
MEIJERE, A. DE, SCHALLNER, O. & WEITEMEYER, C. (1973). *Tetrahedron Lett.* **36**, 3483–3486.
NES, G. J. H. VAN & VAN BOLHUIS, F. (1978). *J. Appl. Cryst.* **11**, 206–207.
NIJVELDT, D. & VOS, A. (1988*a*). *Acta Cryst.* B**44**, 289–296.
NIJVELDT, D. & VOS, A. (1988*b*). *Acta Cryst.* B**44**, 296–307.
REES, B. (1976). *Acta Cryst.* A**32**, 483–488.
STEWART, R. F., BENTLEY, J. & GOODMAN, B. (1975). *J. Chem. Phys.* **63**, 3786–3793.
STEWART, R. F. & SPACKMAN, M. A. (1981). *VALRAY Users Manual.* Preliminary Draft. Department of Chemistry, Carnegie-Mellon Univ., Pittsburgh, PA, USA.
TRÆTTEBERG, M. (1983). Private communication.
WAL, R. VAN DER (1982). PhD Thesis. Univ. of Groningen, The Netherlands.
WILSON, A. J. C. (1976). *Acta Cryst.* A**32**, 781–783.

Acta Cryst. (1988). B**44**, 289–296

Single-Crystal X-ray Geometries and Electron Density Distributions of Cyclopropane, Bicyclopropyl and Vinylcyclopropane. II. Multipole Refinements and Dynamic Electron Density Distributions

BY DICK NIJVELDT AND AAFJE VOS

Laboratory of Chemical Physics, University of Groningen, Nijenborgh 16, 9747 *AG Groningen, The Netherlands*

(*Received* 21 *November* 1986; *accepted* 9 *December* 1987)

Abstract

Multipole refinements have been carried out with the program *VALRAY* to obtain the most accurate models for the geometry and electron density description. During the ultimate multipole refinement on $|F|$, (i) independent reflections weighted with the reflection multiplicity were taken, (ii) extinction corrections were included for bicyclopropyl (BCP) and vinylcyclopropane (VCP), (iii) all available types of multipoles were used for C and H, *viz* up to hexadecapole level, and (iv) the form of the single exponential radial distribution functions for octopoles on C was varied. Final residuals are for cyclopropane (CP) C_3H_6: $R(F) = 0{\cdot}0211$, $R_w(F) = 0{\cdot}0198$; for BCP, C_6H_{10}: $R(F) = 0{\cdot}0210$, $R_w(F) = 0{\cdot}0194$; and for VCP, C_5H_8: $R(F) = 0{\cdot}0159$, $R_w(F) = 0{\cdot}0140$. Pronounced features in the dynamic filtered deformation density distributions are the bent bond character in the plane of the ring and the non-cylindrical distribution around the double bond in VCP.

1. Introduction

A refinement in which account is taken of the nonspherical density distribution of atoms in molecules will render a more realistic model than does a conventional 'spherical-atom' refinement. During these multipole refinements the atomic density functions are taken as rigid and centred on the nuclei. In the present refinements the thermal vibrations are assumed to be harmonic. Experimental $|F|$'s have not been corrected for thermal diffuse scattering. Simple functions have been taken for the radial distributions of the multipoles, because adjustment of complicated functions showing sharp high-resolution features to the observed density is hampered by thermal smearing and limited resolution [van der Wal (1982); refinements on hypothetical SiO having quantum theoretical density affected by thermal smearing and limited resolution].

The electron density distribution is given with respect to the independent atom model (IAM), as a reference. This IAM is chosen as a superposition of the spherically averaged electron densities of atoms p in the

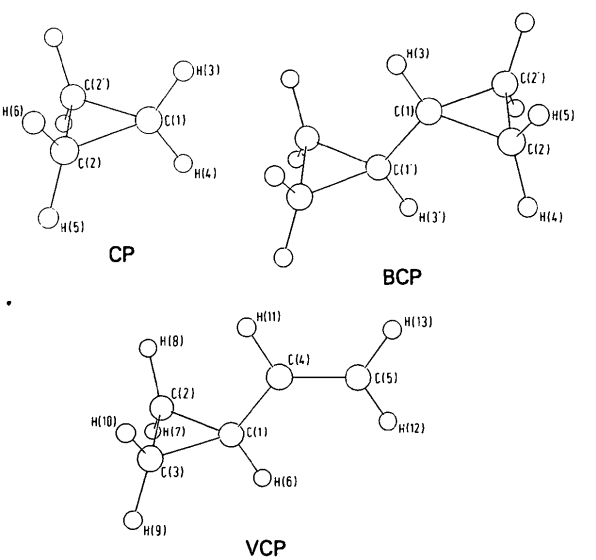

Fig. 1. Atomic numbering in CP, BCP and VCP. Numbers which are related by crystallographic symmetry (paper I, §6), are given as p and p'.

0108-7681/88/030289-08$03.00